TRANSPORT PROBLEMS 2023 Volume 18 Issue 4
PROBLEMY TRANSPORTU DOI:10.20858/tp.2023.18.4.18

Keywords: vibrations; vibratory conveyor; dynamic eliminator; transport stop; feeder; material dosing

Weronika ŻMUDA[1]*, Piotr CZUBAK[2]

OPERATION OF A NEW SINGLE-VIBRATOR CONVEYOR ON THE FALLING SLOPE OF THE SECOND RESONANCE

Summary. The paper presents the possibilities of operating an innovative single-vibrator-driven vibratory conveyor [1] in the vicinity of the second resonance zone. The characteristics of operation on both ascending and descending slopes are presented. The differences in the suspension deflection of the additional mass (which is a dynamic eliminator) during operation before and after the resonance were analyzed. We proposed working on the descending slope of the second resonance in order to increase the durability of the device. This is because the amplitude of the suspension deflection of the additional mass is limited and, due to its high stiffness, is exposed to material fatigue. This is an unusual method of operation for conveyors because it carries certain risks, such as the risk of the device entering resonance on its own or the problem of maintaining constant angular velocity of the unbalanced masses. This paper presents both analytical and simulation studies, which were then confirmed on a laboratory stand designed and built by the authors.

1. INTRODUCTION

Vibratory conveyors play an important role among the devices used for bulk materials transportation. They are used for transport over short distances (i.e., distances not exceeding several tens of meters). Conveyors are used to transport the material along a downward or upward slope in the range of -15° to +15°. The frequency of vibration of the trough of a vibratory conveyor ranges from 10 to 100 Hz and can be sub-resonant, resonant, or over-resonant depending on whether it is less than, equal to, or greater than the natural frequency of the conveyor (if and only if its suspension system on the direction of motion has one degree of freedom). In the case of conveyors with more Degrees of Freedom it can achieve an inter-resonant frequency [2]. The vibration amplitude can range from a few tenths of a millimeter to several millimeters [3].

Inertia-driven conveyors are usually characterized by a system of two self-synchronizing electrovibrators [4–6], resulting in directional force in the direction of motion of the trough. The following paper presents the transport capabilities of a new patent-pending, single-vibrator conveyor. In previous papers, the authors investigated the transport capabilities of the new vibratory conveyor as well as precision dosing and reverse operation in the inter-resonance zone [7]. The problem of dosing was also presented in the paper [8], while the analysis of the dual-mass machine is widely described in [9]. This work presents the operating possibility of the conveyor in a falling slope of the second resonance strongly dependent on the additional mass – an eliminator [10]. Such operation gives the advantage of lowering the amplitude of the eliminator suspended by a stiff suspension system to the trough and, at the same time, is prone to fatigue. An additional advantage of reduced deflection amplitudes of the eliminator's suspension system is that it saves energy used for dissipation in the

[1] AGH University of Krakow; Mickiewicza av. 30, 30-059 Krakow, Poland; e-mail: wezmuda@agh.edu.pl; orcid.org/0000-0002-8632-9266
[2] AGH University of Krakow; Mickiewicza av. 30, 30-059 Krakow, Poland; e-mail: czubak@agh.edu.pl; orcid.org/0000-0001-8030-7173
*_Corresponding author_. E-mail: wezmuda@agh.edu.pl

eliminator's suspension. It should be remembered that operation in this frequency range carries dangers in the form of difficulty in maintaining constant angular velocity of unbalanced masses as well as the danger of entering the resonance zone.

2. SCHEME AND OPERATION PRINCIPLE OF THE CONVEYOR

The scheme of the conveyor is presented in Fig. 1a, and the real device built from industrial parameters is shown in Fig. 1b.

a)

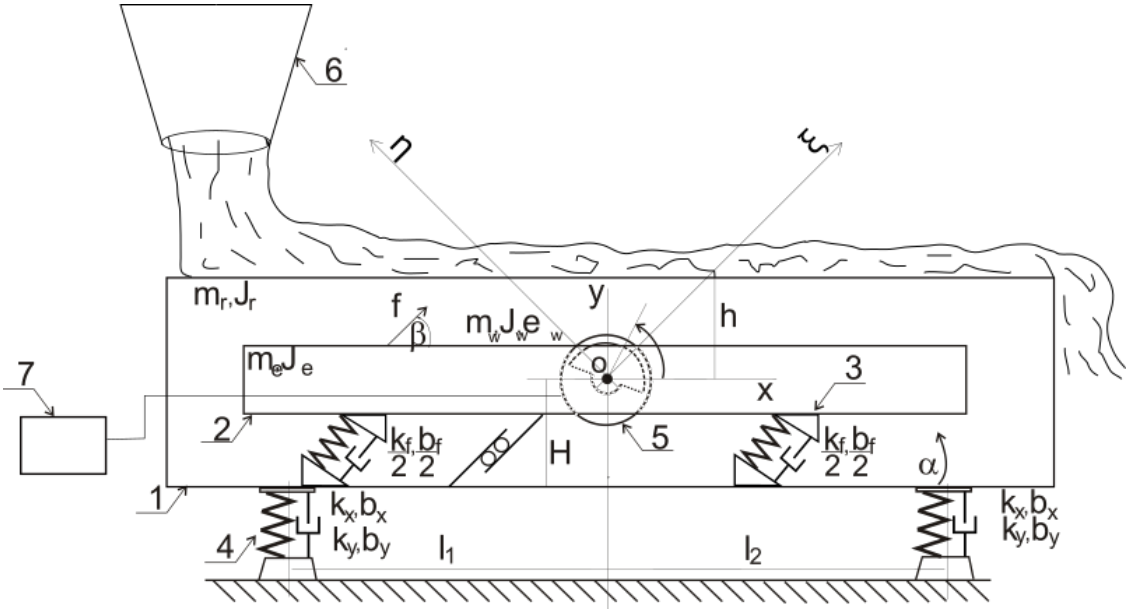

b)

Fig. 1. a) scheme of the conveyor and b) the real device

The conveyor is equipped with one electrovibrator (5) powered by an inverter (7). Transport occurs due to vibration excitation in the working direction by means of an additional mass (2), which is

connected to the trough (1) by a suspension system (4). In a classic conveyor positioned on an omni-directional suspension, there is a need for a directional forcing (e.g., two synchronized vibrators) [11,12], which excites the trough to vibrate at a certain angle to the horizontal axis. In this case, the vibrator causes a force in each direction in the axis of its rotation. Since the excitation force is relatively small (10 times smaller than in a typical conveyor with the same parameters) [13], the excitation of vibrations is very small in the η direction [14]. However, in the ξ direction, significant excitation of vibrations occurs because the additional mass (2) works in this direction due to the system of strip springs (3). The above considerations refer to the operation of the device in the vicinity of the second resonance zone.

The parameters presented in Tab. 1 [7] are the values corresponding to the machine introduced in Fig. 1. Values, such as the masses of the main elements and the parameters of the suspension systems, were initially selected at the design stage of the conveyor. They were later verified on the laboratory stand. The only parameters that were not corrected in relation to those determined from technical drawings were moments of inertia of the main masses and the bearing resistance coefficient. These values were estimated based on tabular data and the authors' experience.

Table 1

Parameters of the model used for simulation

Symbol	Value	Unit	Description
$l_1 = l_2$	0.365	m	Distance between the center of rotation and the axis of a spring
$b_x = b_y$	58	Ns/m	Damping coefficient of the coil spring
$k_x = k_y$	32000	N/m	Stiffness coefficient of the coil spring
b_f	40	Ns/m	Strip springs damping coefficient
k_f	937367	N/m	Strip springs stiffness coefficient
m_e	42.5	Kg	Additional mass's weight
m_r	65	Kg	Trough's mass
m_w	6	Kg	Total mass of unbalance
J_e	3.7	kgm^2	Moment of inertia of the eliminator
J_r	4.82	kgm^2	Moment of inertia of the trough
J_w	0	kgm^2	Moment of inertia of the unbalanced mass
β	45	°	Working angle of the strip springs
e	0.003	M	Eccentricity
m_{ut}	4.26	Nm	Maximum torque
b_s	0.00009	Ns^2/m	Bearing resistance coefficient

Assuming that the stiffness and damping coefficients in the x and y directions are similar, the system can be represented by a diagram (Fig. 2).

The equation in the direction of η:

$$(m_r + m_e)\ddot{\eta} + b_y\dot{\eta} + k_y\eta = F_0(t) \tag{1}$$

Equations in the direction of ξ:

$$m_e\ddot{f} + b_f(\dot{f} - \dot{y}) + k_f(f - y) = F_0(t) \tag{2}$$

$$m_r(\ddot{y}) - b_f(\dot{f} - \dot{y}) + b_y\dot{y} - k_f(f - y) + k_y y = 0 \tag{3}$$

For a monoharmonic driving force in the form:

$$F_0(t) = m_w e\omega^2 \sin\omega t \tag{4}$$

and restricting to the steady-state, the system of differential equations can be reduced to the following forms:

For system no. 1:

$$-(m_e + m_r)\omega^2 \underline{H} + b_y i\omega \underline{H} + k_y \underline{H} = m_w e\omega^2 \tag{5}$$

For system no. 2:

$$-m_e\omega^2 \underline{F} + b_f i\omega\left(\underline{F} - \underline{Y}\right) + k_f\left(\underline{F} - \underline{Y}\right) = m_w e\omega^2 \tag{6}$$

$$-m_r\omega^2 \underline{Y} + b_f i\omega\left(\underline{Y} - \underline{F}\right) + b_y i\omega \underline{Y} + k_f\left(\underline{Y} - \underline{F}\right) + k_y \underline{Y} = 0 \tag{7}$$

where:

$\underline{Y}$ - amplitude of harmonic motion along the coordinate y,
$\underline{F}$ - amplitude of harmonic motion along the coordinate f,
$\underline{H}$ - amplitude of harmonic motion along the coordinate η,
ω - angular frequency of the excitation force $F_0(t)$, and
i - imaginary unit.

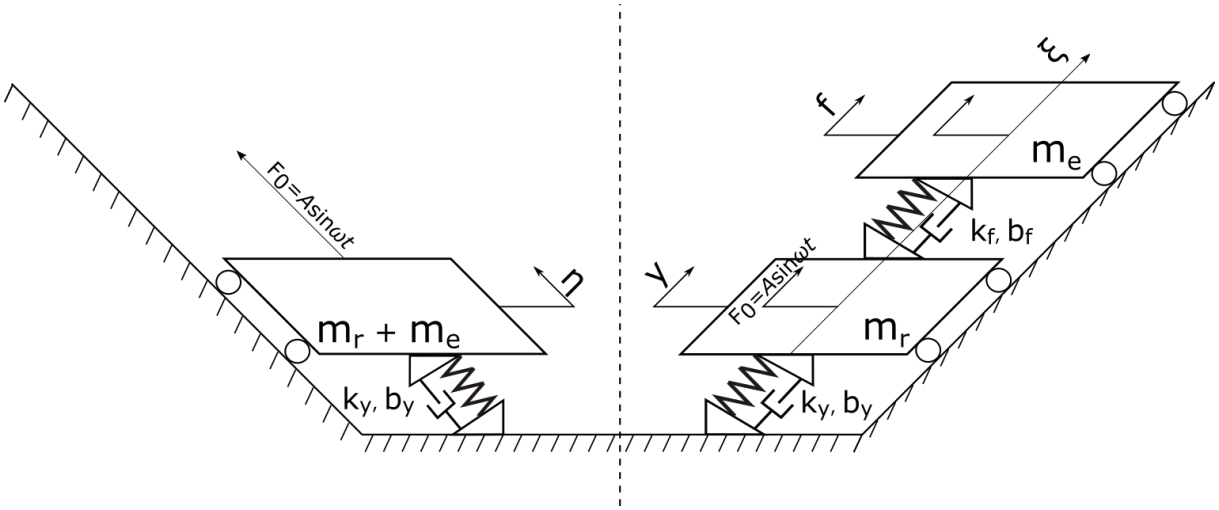

Fig. 2. Motion analysis of the analytical model in two perpendicular directions – a one-mass system in the direction (system no. 1) and a two-mass system in the ξ direction (system no. 2)

After solving these equations with unknowns Y and F, complex values of the amplitudes are given:
For system no. 1:

$$\underline{H} = \frac{m_w e\omega^2}{(m_r + m_e)\omega^2 - k_y - ib_y\omega} \tag{8}$$

For system no. 2:

$$\underline{F} = \frac{-m_w e\omega^2\left(m_r\omega^2 - i\left(b_f - b_y\right)\omega - \left(k_f + k_y\right)\right)}{\left(m_e m_r\omega^4 - m_e\omega^2\left(k_y + k_f\right) - m_r\omega^2 k_f + k_y k_f - b_y b_f\omega^2\right) - i(m_e\omega^3\left(b_y + b_f\right) - k_f b_y\omega + m_r\omega^3 b_f - b_f k_y\omega)} \tag{9}$$

$$\underline{Y} = \frac{m_w e\omega^2(ib_f\omega + k_f)}{\left(m_e m_r\omega^4 - m_e\omega^2\left(k_y + k_f\right) - m_r\omega^2 k_f + k_y k_f - b_y b_f\omega^2\right) - i(m_e\omega^3\left(b_y + b_f\right) - k_f b_y\omega + m_r\omega^3 b_f - b_f k_y\omega)} \tag{10}$$

Considering the vibrations in the η and ξ directions, the diagrams shown in Fig. 3 are given. The outcome for the η direction concerns the mass that is the sum of the eliminator's and trough's masses. For the ξ direction, vibrations of masses for the eliminator and trough are considered separately.

Fig. 3a [7] shows the dependence of vibrations on the excitation frequency in the η direction. It is seen that after passing through the first resonance zone, the trough has a constant amplitude at a low magnitude, which in turn does not affect the transport of material. This is due to the fact of acting with low force. In the direction of ξ (Fig. 3b), trough vibrations pass through the first resonance; then,

together with an increase of the angular velocity – trough vibrations pass through the anti-resonance zone in which it's vibration disappear what causes the stop of transportation [7]. Later, the device passes through the second resonance and, together with a further increase in the excitation frequency, the vibrations stabilize. Authors have analyzed the operation of the device on the leading slope of the second resonance in the previous work. Such operation allows the transport to be stopped by reducing the excitation frequency to the anti-resonance frequency (Fig. 3b). This provides the opportunity to dose the material using the conveyor. For the operation point set right before the anti-resonance, the amplitude of deflection of the eliminator's suspension is higher than the nominal amplitude of the trough. This is unfavorable due to the fatigue of the eliminator's suspension, which, due to the characteristics of the device, must be rigid, and for construction reasons, it must also be strip springs. Such a type of spring is characterized by lower strength due to fatigue. If the conveyor is used for material transportation continuously instead of dosing it, there is a possibility of working on the falling slope of the second resonance zone (Fig. 3c).

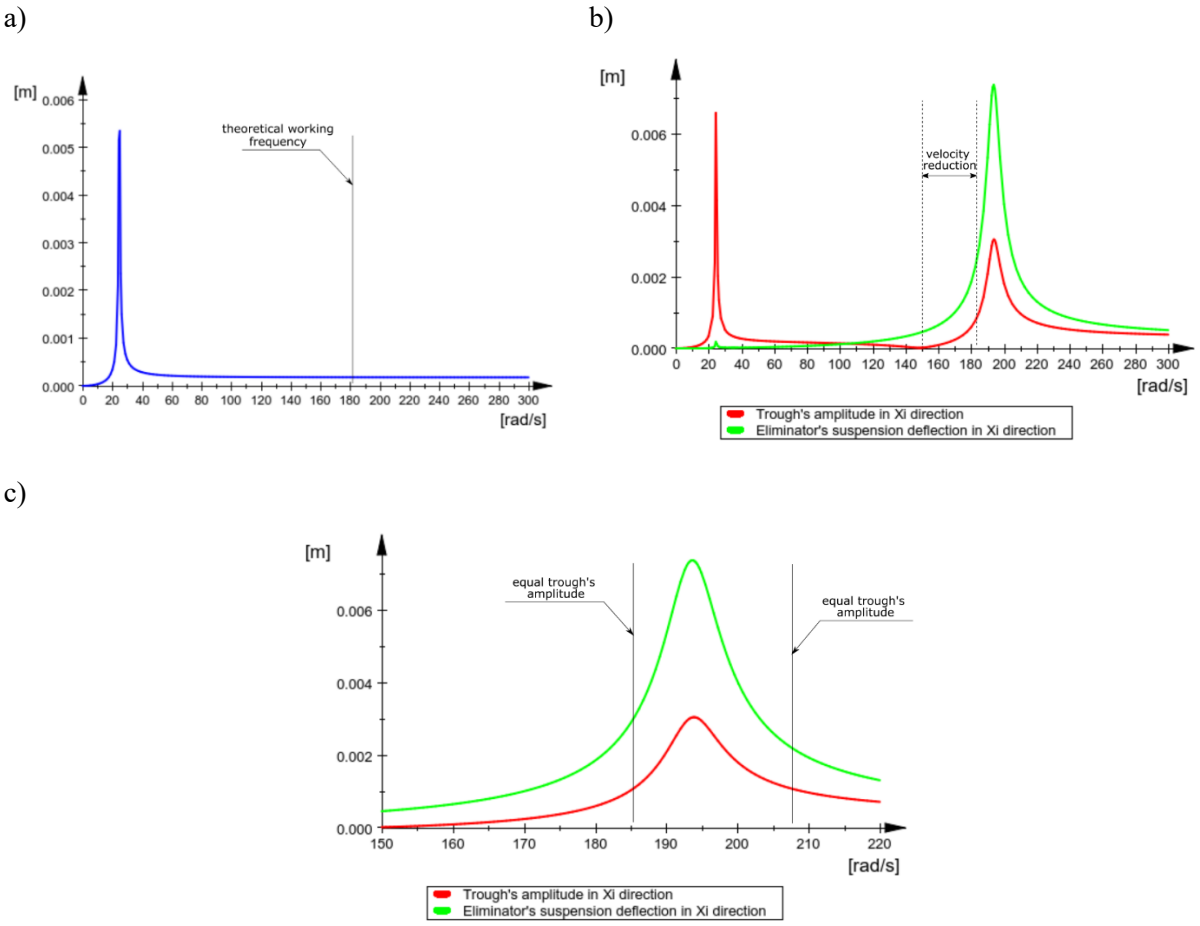

Fig. 3. Amplitudes for reduced unbalance a) for the trough in η direction, b) for the device in ξ direction, and c) for the device in ξ direction in the second resonance zone

Such operation is advantageous because it reduces the deflection amplitude of the spring strips while keeping the trough amplitude constant. For the trough amplitude of 1.13 mm, the deflection amplitude of the eliminator's suspension before the second resonance is 3.75 mm, while it is 2.6 mm behind the zone. In terms of absolute numbers, a reduction of suspension deflection of 31% does not seem significant. However, considering a Woehler fatigue diagram for steel [15], such a reduction significantly extends the durability of the spring strips. In addition to reducing the risk of material fatigue of the suspension, the advantage of such operation is that it reduces the energy dissipation in the suspension system of the additional mass. Some problems can arise with such an operation. These

are the unstable angular velocity of the unbalanced masses and the danger of the drive getting stuck during start-up when passing through the second resonance, which is very close to the operating point.

3. MATHEMATICAL MODEL

A model of the device [7] was used to investigate the transport possibility of the machine at the operating point (behind the second resonance).

In the paper [7], the authors considered the feed being transported on the trough of the conveyor. In the following paper, the influence of the feed was neglected because the amount of feed transported on the trough was limited during the operation of the author's conveyor on the descending slope of the second resonance. Operation in this zone causes the conveying speed to drop significantly when the trough is heavily loaded. The conveyor in the analyzed zone works correctly only for a light load of the trough in relation to its mass. Light loads are those that do not exceed 20% of the trough's mass.

The mathematical model of the system contains the matrix equation describing the machine motion (11), consisting of the mass matrix (12) and force matrix (14), as well as equations concerning the electromagnetic moment of the drive motor (15).

$$\boldsymbol{M} \cdot \ddot{\boldsymbol{q}} = \boldsymbol{Q} \tag{11}$$

$$\boldsymbol{M} = \begin{bmatrix} m_r + m_w + m_e & 0 & 0 & m_w e \sin\varphi & m_e \cos\beta \\ 0 & m_r + m_w + m_e & m_w e \cos\varphi & m_w e \cos\varphi & m_e \sin\beta \\ 0 & 0 & J_r + J_e & 0 & 0 \\ m_w e \sin\varphi & m_w e \cos\varphi & 0 & m_w e^2 + J_w & 0 \\ m_e \cos\beta & m_e \sin\beta & 0 & 0 & m_e \end{bmatrix} \tag{12}$$

$$\ddot{\boldsymbol{q}} = [\ddot{x} \quad \ddot{y} \quad \ddot{\alpha} \quad \ddot{\varphi} \quad \ddot{f}]^T \tag{13}$$

$$\boldsymbol{Q} = \begin{bmatrix} -m_w e \varphi^2 \cos\varphi - 2k_x(x + H\alpha) - 2b_x(\dot{x} + H\dot{\alpha}) \\ m_w e \varphi^2 \sin\varphi - k_y(y + l_1\alpha) - k_y(y - l_2\alpha) - b_y(\dot{y} + l_1\dot{\alpha}) - b_y(\dot{y} - l_2\dot{\alpha}) \\ -2k_x H^2\alpha - 2k_x Hx - 2b_x H\dot{x} - 2b_x H^2\alpha - k_y(y + l_1\alpha)l_1 + k_y(y - l_2\alpha)l_2 - b_y(\dot{y} + l_1\dot{\alpha})l_1 + b_y(\dot{y} - l_2\dot{\alpha})l_2 \\ M_{el} - b_s\dot{\varphi}\sin\varphi \\ -k_f f - b_f\dot{f} \end{bmatrix} \tag{14}$$

Kloss's equation (15) is used as far as the mechanical characteristics of the asynchronous engine are concerned:

$$M_{eli} = \frac{2M_{ut}(\omega_{ss} - \dot{\varphi}_i)(\omega_{ss} - \omega_{ut})}{(\omega_{ss} - \omega_{ut})^2 + (\omega_{ss} - \dot{\varphi}_i)^2} \tag{15}$$

where:

M_{eli} - electromagnetic moment developed by motor i, assumed to be in a form corresponding with the static characteristic of a motor

M_{ut} - stalling torque of drive motors,

ω_{ss} - synchronous frequency of drive motors,

ω_{ut} - frequency of stall of drive motors.

4. SIMULATION AND EXPERIMENTAL RESULTS

The graphs below (Figs. 4a and 4b) show the quasi-state amplitude of the vibrations of the trough and the deflection amplitude of the eliminator's suspension for varying excitation frequency. The nominal amplitude of the trough equal to 1.13 mm is marked in the figures in the second resonance zone. Corresponding magnitudes of the eliminator's suspension deflection amplitudes are also marked in the graphs ('threshold'). Before the resonance zone, it is equal to 3.75 mm; after the resonance zone, it is 2.6 mm.

Experimental tests were performed on the laboratory stand with industrial parameters in order to confirm the analytical and simulation studies. The tests were carried out using a dynamic signal analyzer CoCo (Fig. 5). Fig. 6 presents the vibration amplitudes of the trough and the deflection amplitudes of the eliminator's suspension in the second resonance zone. The considered zone is associated with the additional mass and its suspension system. It should be pointed out that the conveyor is equipped with an additional bumper that does not allow sudden increase of the vibration amplitudes of the eliminator in order for the vibratory conveyor to pass through the resonance zone freely.

a)

b)

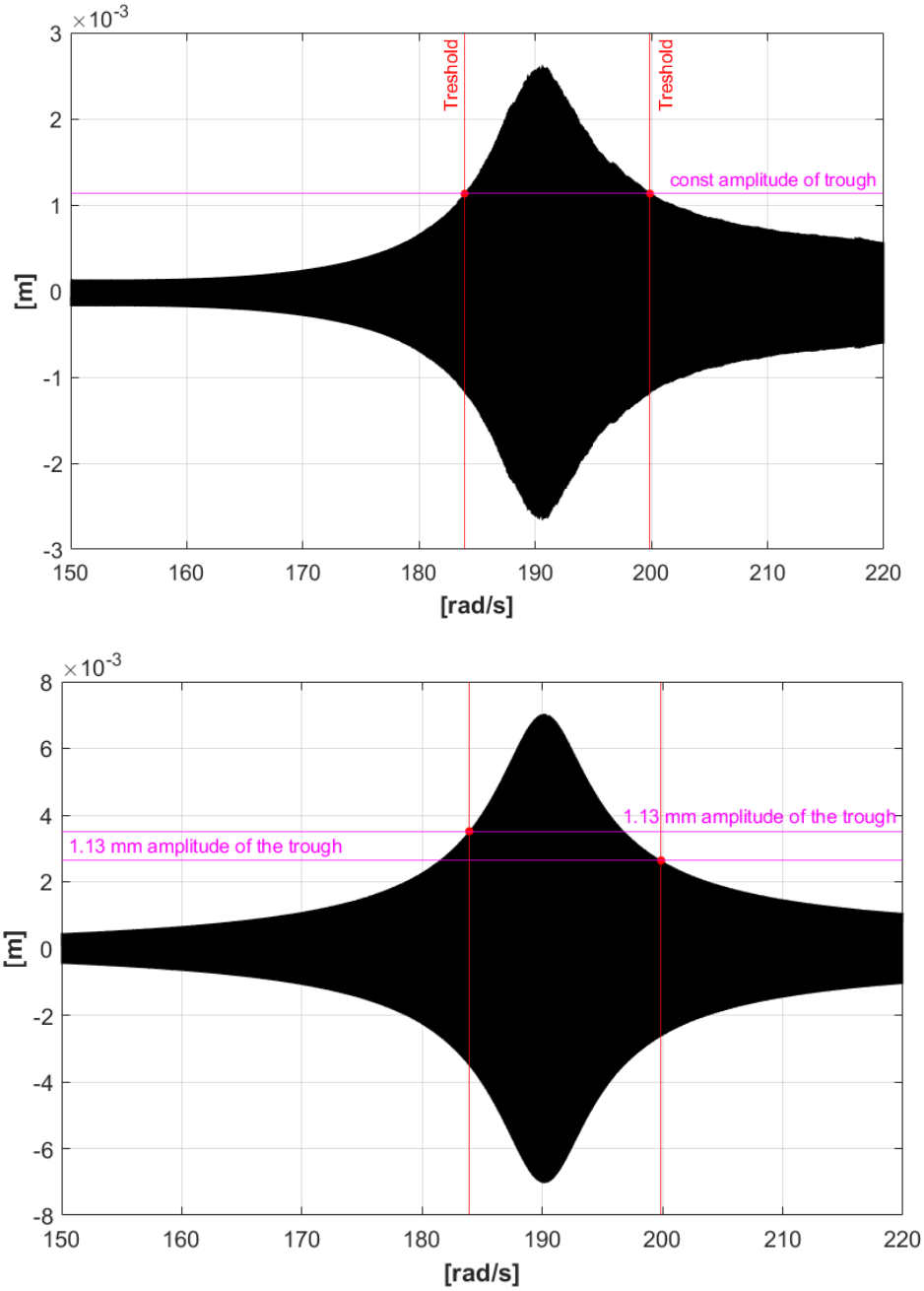

Fig. 4. a) Quasi-state amplitudes of the trough in the ξ direction nearby resonance zone associated with the additional mass b) quasi-state amplitudes of the eliminator's suspension in the ξ direction

The bumper also reduces the risk that the device will get stuck in resonance and protects the eliminator's suspension against damage. Therefore, the amplitudes in the zone between 183 rad/s and 200 rad/s are not measured. As presented in the graphs for the amplitude of the trough corresponding to the working amplitude before and after the resonance zone, a significant reduction of the vibration amplitude of the eliminator is obtained. Such a deflection reduction protects the suspension system from fatigue damage. The results of the measurements confirm the thesis of the paper. Additional tests (not included in the paper) performed on the laboratory stand show a large variation in the speed of the transported material when operating on the descending slope of the resonance. This, in turn, limits the suitability of this type of conveyor setting for lightweight feeds.

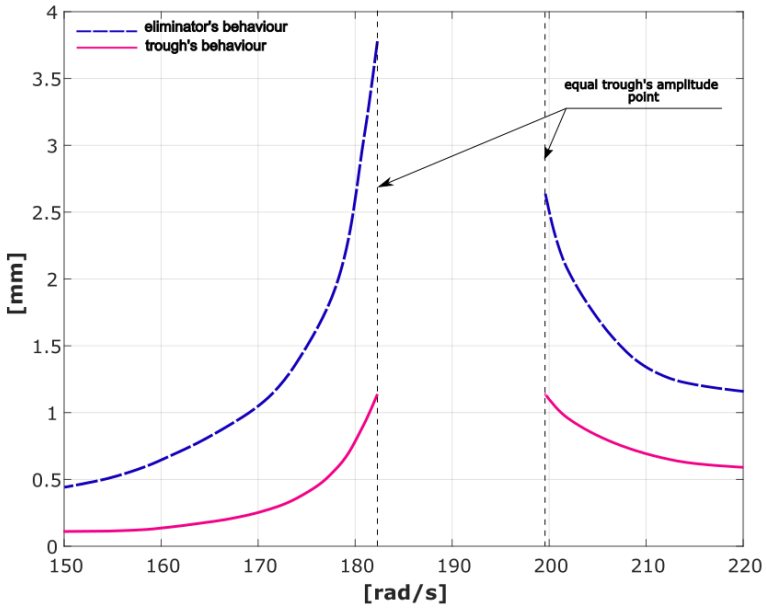

Fig. 5. Results of the amplitude analysis based on experiments performed on the laboratory stand

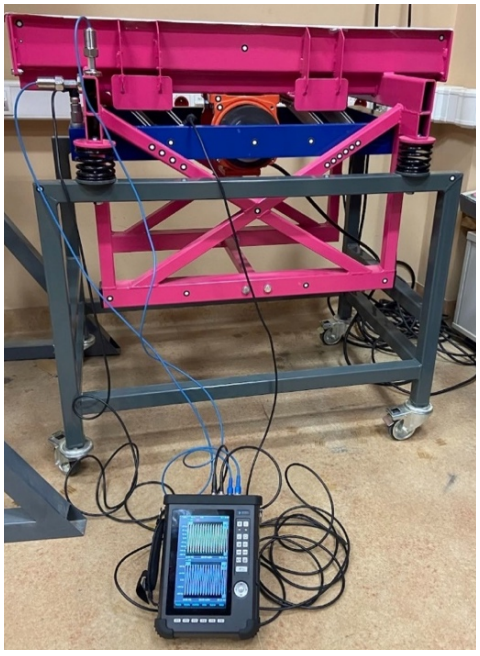

Fig. 6. Test carried out on the laboratory stand with the dynamic signal analyzer CoCo

5. CONCLUSIONS

An analytical analysis of the proposed device shows that it is possible to reduce the deflection amplitudes of the eliminator's suspension by operating in the zone behind the second resonance. Simulation analysis of the model of the new conveyor with five DOF confirmed the possibility of reducing the deflection amplitudes of the eliminator's suspension. Tests carried out on the industrial-sized laboratory stand confirmed the possibility of reducing the deflection amplitudes of the eliminator's suspension in the falling slope of the second resonance. The differences in the values of the eliminator's suspension amplitudes at a constant trough's amplitude of 1.13 mm before and after the resonance zone for different test methods do not exceed 30%. Moreover, analysis shows a reduction in the deflection amplitude in the falling slope of the second resonance. The differences result from the complexity of the analyzed system. However, the differences between the simulation system and the real stand may be due to the inaccurate identification of the parameters of the main suspension and eliminator's suspension system, which has a significant effect in the resonance zone. Tests conducted on the laboratory stand show that the deflection amplitudes of the additional mass's suspension in the falling slope of the resonance zone are 69% of the amplitude before the resonance. Due to fatigue strength, this provides the possibility of significantly increasing the durability of the device.

Acknowledgments

The work is included in the framework of the Department of Mechanics and Vibroacoustics. 16.16.130.942

References

1. Patent Application no. 441218. Żmuda, W. & Czubak, P. *Dispensing Vibratory Conveyor with Reversing Operation Function.* 2022.
2. US989958A. Frahm, H. *Device for Damping Vibrations of Bodies*. 1909.
3. Yeleukulov, Y. & Atalykova, A. & Zhauyt, A. & Abdimuratov, Z. & Yussupova, S. & Alik, A. & et al. Mechanical analysis of vibratory conveyor mechanism. In: *MATEC Web of Conferences.* 2018.
4. Sturm, M. *Design Optimization of Linear Vibratory Conveyors.* PhD thesis. Liberec. Technical University of Liberec. 2018.
5. Sturm, M. Two-mass linear vibratory conveyor with reduced vibration transmission to the ground. *Vibroengineering Procedia*. 2017. Vol. 13. Available at: https://www.extrica.com/article/19066/pdf
6. Blekhman, I. *Synchronization in Science and Technology*. NY: ASME Press. 1988.
7. Żmuda, W. & Czubak. P. Study of transport possibilities in the resonance zone of the new vibratory conveyor equipped with the single electro-vibrator. *Vibrations in Physical Systems.* 2023. No. 2023116.
8. Zejer, T. & Olesiński, M. & Musioł, K. & Okoń, T. Stopping Material Transport on Vibrating Feeder Chute. In: *International Colloquium Dymamesi 2021 - Dynamics of Machines and Mechanical Systems with Interactions*. Krakow. Poland. 2021.
9. Despotovic, Z.V. & Stojiljkovic, Z.V. PSPICE simulation of two-mass vibratory conveying system with electromagnetic drive. In: *EUROCON 2005 - The International Conference on Computer as a Tool*. 2005.
10. Jiao, C.W. & Liu. J. & Wang, Q.Q. Dynamic analysis of nonlinear anti-resonance vibration machine based on general finite element method. *Advanced Materials Research*. 2012. Vols. 443-444. P. 694-699.

11. Nendel, K. & Risch, T. Two-dimensional movement patterns of vibratory conveyors. *Logistics Journal Referierte Veröffentlichungen*. 2010. Available at: https://www.logistics-journal.de/archive/2010/2672/Nendel_Risch_Eng.pdf
12. Buzzoni, M. & Battarra, M. & Mucchi, E. & Dalpiaz, G. Motion analysis of a linear vibratory feeder: Dynamic modeling and experimental verification. *Mech Mach Theory*. 2017. Vol. 114. P. 98-110.
13. Korendiy, V. & Kachur, O. & Dmyterko, P. Kinematic analysis of an oscillatory system of a shaking conveyor-separator. *Lecture Notes in Mechanical Engineering*. 2022. P. 592–601.
14. Lim, G.H. On the conveying velocity of a vibratory feeder. *Comput Struct*. 1997. Vol. 62(1). P. 197-203.
15. Kocańda, S. & Szala, J. *Podstawy obliczeń zmęczeniowych*. Wydanie trzecie zmienione. Warszawa. Wydawnictwo Naukowe PWN. 1997. [In Polish: *Fundamentals of fatigue calculations.* 3rd ed.].

Received 01.07.2022; accepted in revised form 04.12.2023